Heat Transfer Investigation of TiO_2 Nanofluid in Silica Aerogel/Glass Fiber Composite Material Enclosure

Manal H. AL- Hafidh
Department of Mechanical Engineering

Khawla A. AL Zubaidy
Department of Mechanical Engineering

ABSTRACT
This research investigates the natural convection heat transfer of nanofluid taking the water as based fluid withTiO_2 nano particles in an annulus enclosure of a three dimension filled with silica sand as porous media between two horizontal concentric cylinders. Fins attached to the inner cylinder and steady state conditions are applied. The finite difference approach is used and the results obtained using the MATLAB program. The parameters affected on the system are modified Rayleigh number ($10 \le Ra^* \le 800$), cylinders radius ratio Rr (0.293, 0.365 and 0.435) and the volume fraction $(0 \le \varphi \le 0.5)$. It was found that the increase of Ra^* and/or decrease in radius ratio result an increase in heat transfer. For cold cylinder with Ra^*=800, adding TiO_2 nanoparticles of a volume fraction equal 0.5 cause to increase the average Nu by 450% for Rr=0.293 and 519.6 % increase in average Nu for Rr=0.365 and for Rr=0.435 the % increase in the average Nu is 536.33. Effect of nanoparticles on enhancement of heat transfer at high Ra^* is more significant than that at low Ra^*.

General Terms
Cp: Specific heat at constant pressure (kJ/kg ^{o} C), g: Acceleration due to gravity (m/s^2), kf: Thermal conductivity of the fluid (W/m K), ks: Thermal conductivity of the solid (W/m K), keff.: Effective thermal conductivity of the porous media (W/m K), K: Permeability (m^2), l: Cylinder length (m), L:Dimensionless cylinder length, Nu1: Local Nusselt number on the inner cylinder, Nu2: Local Nusselt number on the outer cylinder, Nu_{in}: Average Nusselt number on the inner cylinder, Nu_{out}: Average Nusselt number on the outer cylinder, p: Pressure (N/m2), q: Local heat flux (m), r: Radial coordinate (m), R: Dimensionless radial coordinate, Ra*: Modified Rayleigh number, Rr: Radius ratio, S: Fin pitch (m), T: Temperature (K), t: time (s), ur,uϕ, uz: velocity component in r,ϕ and z - direction (m/s), Ur, Uϕ, Uz: Dimensionless velocity component in R, ϕ and Z direction, x, y, z: Cartesian coordinate system (m), Z: Dimensionless axial coordinate, α: Thermal diffusivity (m^2/s), β: Volumetric thermal expansion coefficient (1/K), θ: Dimensionless temperature, ψr, ψϕ, ψz: Vector potential component in R,ϕ and Z – direction**,** μ_f **:** Dynamic viscosity of fluid (Pa.s), μ_{nf} Dynamic viscosity of nanofluid(Pa.s), FAI**:** angular direction**.**

Keywords
Laminar free convection, TiO_2 Nanofluid, Porous media, Horizontal annulus.

1. INTRODUCTION
Due to the importance of engineering applications such as solar collectors, geothermal and oil recovery, drying processes, heat exchangers, building construction, which is concerned with the natural convective flow in porous media, many books were written, contains practical problems of the applications of porous media as in [1], [2] and [3]. The heat transfer and fluid flow was studied due to buoyancy forces in a partially heated enclosure using nanofluids of different nanoparticles types [4]. The researcher used the finite volume technique to solve the governing equations. The affected parameters are Rayleigh number ($10^3 \le Ra \le 5 \times 10^5$), height of heater ($0.1 \le h \le 0.75$), location of heater ($0.25 \le yp \le 0.75$), aspect ratio ($0.5 \le A \le 2$) and volume fraction of nanoparticles ($0 \le \varphi \le 0.2$). The results show an increase in mean Nusselt number with the volume fraction of nanoparticles for all the ranges of Rayleigh number. Also increasing the height of the heater causes to increase heat transfer. It was found that the heater location affects the flow and temperature fields when using nanofluids and that the heat transfer enhancement, using nanofluids, is more pronounced at low aspect ratio than at high aspect ratio.

A boundary layer analysis is presented for the natural convection heat transfer past a vertical flat plate embedded in a porous medium filled with nanofluids by [5] and past along two different geometries i.e., a vertical cone and an isothermal sphere in a Non-Darcy porous medium saturated with a nanofluid. [6] Presented the steady fully developed mixed convection flow of a nanofluid in a channel filled with a porous medium.

Heat transfer enhancement utilizing nanofluids in a trapezoidal enclosure is investigated by [7]. For various parameters, governing equations are modeled by a stream-vorticity formulation and solved numerically by finite difference approach. The inclined sloping boundaries are treated by adopting staircase- like zigzag lines. Water–Cu and water–Al2O3 nanofluids were tested. The results show that acute sloping wall and Cu nanoparticles with high concentration are effective to enhance the rate of heat transfer.

For both cases of a heated and cooled cylinder, [8] studied the steady mixed convection boundary layer flow from an isothermal horizontal circular cylinder embedded in a porous medium filled with a nanofluid. Laminar conjugate heat transfer by natural convection and conduction in a vertical annulus formed between an inner heat generating solid circular cylinder and an outer isothermal cylindrical boundary has been studied by a numerical method [9]. The governing equations have been solved using the finite volume approach, using SIMPLE algorithm on the collocated arrangement. The parameters affected are Ra (10^5 to 10^8), solid volume fraction of $0<\varphi<0.05$ with copper-water nanofluid as the working medium. The study has been carried out for different inclination angles. The effects of Grashof number and volume fraction of Cu-water nanofluid on natural convection heat transfer and fluid flow inside a two-dimensional wavy enclosure is studied numerically by [10]. Calculations were performed for the Gr (10^4 to 10^6), surface waviness ranging from 0.0 to 0.4 for different patterns of wavy enclosure

nanoparticles and volume fraction from 0% to 10%. Finite-Volume numerical procedure is used to solve the governing differential equations.

For the present research, the natural convection heat transfer of nanofluid taking the water as based fluid withTiO_2 nano particles in an annulus enclosure of a three dimension filled with silica sand as porous media between two horizontal concentric cylinders is investigated. The schematic drawing of the geometry and the Cartesian coordinate system employed in solving the problem is shown in **Fig.1**.

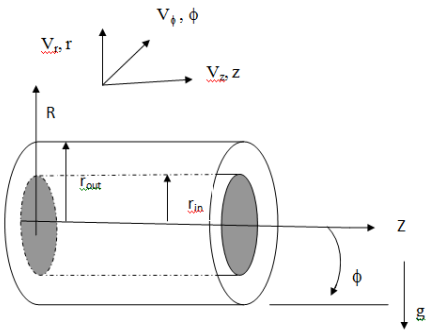

Fig.1 Geometry and coordinates system

2. MATHEMATICAL MODEL

The Maxwell-Garnetts model of effective thermal conductivity of the nano-fluid is approximated as:

$$\frac{k_{nf}}{k_f}=\frac{k_s+2k_f-2\phi\left(k_f-k_s\right)}{k_s+2k_f+\phi\left(k_f-k_s\right)} \tag{2.1}$$

This model is found to be appropriate for studying heat transfer enhancement using nanofluid [9, 10]. This equation is used for spherical nano-particles where it does not account for other shapes of nano-particles. The viscosity of the nano-fluid can be approximated as viscosity of a base fluid μ_f containing dilute suspension of fine spherical particles and is given by [11]:

$$\mu_{nf}=\frac{\mu_f}{(1-\phi)^{2.5}} \tag{2}$$

The governing equations used are continuity, momentum and energy equations which are transformed to dimensionless equations and the vector potential equation is obtained in the dimensionless form as [12]and [13]:

$$\frac{\partial U_r}{\partial R}+\frac{U_r}{R}+\frac{1}{R}\frac{\partial U_\phi}{\partial\phi}+\frac{\partial U_z}{\partial Z}=0 \tag{1}$$

$$Ra^*\,\mathrm{Pr}*C_1*\left(\sin\phi\,\frac{\partial\theta}{\partial Z}\right)=$$
$$-\frac{\partial^2\psi_r}{\partial R^2}-\frac{1}{R^2}\frac{\partial\left(R\psi_r\right)}{\partial R}-\frac{2}{R}\frac{\partial\psi_r}{\partial R}-\frac{1}{R^2}\frac{\partial^2\psi_r}{\partial\phi^2}$$
$$-\frac{\partial^2\psi_r}{\partial Z^2}-\frac{2}{R}\frac{\partial\psi_z}{\partial Z} \tag{2.2}$$

$$Ra^*\,\mathrm{Pr}\;C_1*\left(\cos\phi\,\frac{\partial\theta}{\partial Z}\right)=$$
$$-\frac{\partial^2\psi_\phi}{\partial Z^2}-\frac{\partial^2\psi_\phi}{\partial R^2}-\frac{1}{R^2}\frac{\partial^2\psi_\phi}{\partial\phi^2}$$
$$-\frac{2}{R^2}\frac{\partial\psi_r}{\partial\phi}+\frac{\psi_\phi}{R^2}-\frac{1}{R}\frac{\partial\psi_\phi}{\partial R} \tag{2.3}$$

$$-\frac{Ra^*\,\mathrm{Pr}\;C_1}{\alpha_{nf}}\left(\frac{1}{R}\cos\phi\frac{\partial\theta}{\partial\phi}+\sin\phi\frac{\partial\theta}{\partial R}\right)=$$
$$-\frac{\partial^2\psi_z}{\partial R^2}-\frac{1}{R}\frac{\partial\psi_z}{\partial R}$$
$$-\frac{1}{R^2}\frac{\partial^2\psi_z}{\partial\phi^2}-\frac{\partial^2\psi_z}{\partial Z^2} \tag{2.4}$$

Where $C_1=\frac{\alpha_f}{\alpha_{nf}}\left[(1-\varphi)+\varphi\frac{(\rho\beta)_s}{(\rho\beta)_f}\right](1-\varphi)^{2.5}$

And the energy equation will be:

$$\left(\frac{1}{R}\frac{\partial\psi_z}{\partial\phi}-\frac{\partial\psi_\phi}{\partial Z}\right)\frac{\partial\theta}{\partial R}+\frac{1}{R}\left(\frac{\partial\psi_r}{\partial Z}-\frac{\partial\psi_z}{\partial R}\right)\frac{\partial\theta}{\partial\phi}$$
$$+\left(\frac{\psi_\phi}{R}+\frac{\partial\psi_\phi}{\partial R}-\frac{1}{R}\frac{\partial\psi_r}{\partial\phi}\right)\frac{\partial\theta}{\partial Z} \tag{2.5}$$
$$=\frac{\alpha_{nf}}{r_2}\left[\frac{\partial^2\theta}{\partial R^2}+\frac{1}{R}\frac{\partial\theta}{\partial R}+\frac{1}{R^2}\frac{\partial^2\theta}{\partial\phi^2}+\frac{\partial^2\theta}{\partial Z^2}\right]$$

And fin equation will be [14]:

$$\frac{\partial\theta}{\partial R}+\frac{\theta}{R}+\frac{1}{R}\frac{\partial\theta}{\partial\phi}+\frac{\partial\theta}{\partial Z}=0 \tag{2.6}$$

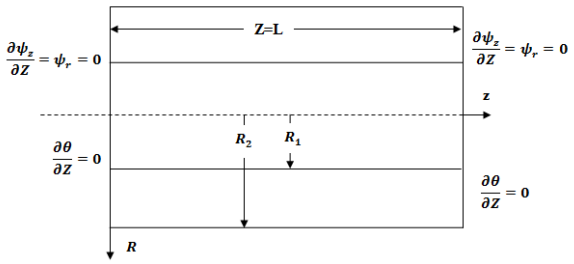

Annulus boundary conditions

Fig. 2. illustrates the vector potential field with the boundary conditions

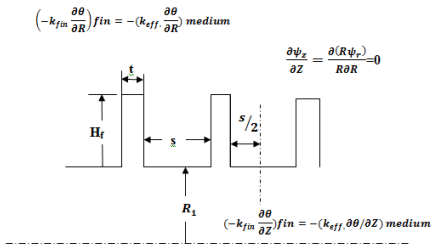

Fin Boundary Conditions

Fig. 2 Annulus and fins boundary conditions

3. COMPUTATIONAL TCHNIQUE

The equations are transformed to the finite difference approximation, applying the upwind differential method in the left hand side of the energy equation and the centered – space differential method for the other terms and solved by using (SOR) method [12]. A mat lab computer program was built to meet the requirements of the problem. The value of the vector potential ψ calculated at each node, in which the value of vector potential is unknown, the other node will appear in the right hand side of each equation. The number of grid points used was 21 grid points in the R – direction, 31 in the ϕ – direction and 301 in the Z – direction.

4. CALCULATION OF AVERAGE NUSSELT NUMBER

The average Nusselt number Nu_{hot} and Nu_{cold} on the inner and the outer cylinders are defined as:

$$Nu_{hot} = -(1-R_1)\frac{k_{nf}}{k_f}\frac{1}{\pi L}\int_0^L\int_0^\pi\left(\frac{\partial\theta}{\partial R}\right)_{R=R} d\phi\, dZ \qquad (7)$$

$$Nu_{cold} = -(1-R_1)\frac{k_{nf}}{k_f}\frac{1}{\pi L}\int_0^L\int_0^\pi\left(\frac{\partial\theta}{\partial R}\right)_{R=1} d\phi\, dZ \qquad (8)$$

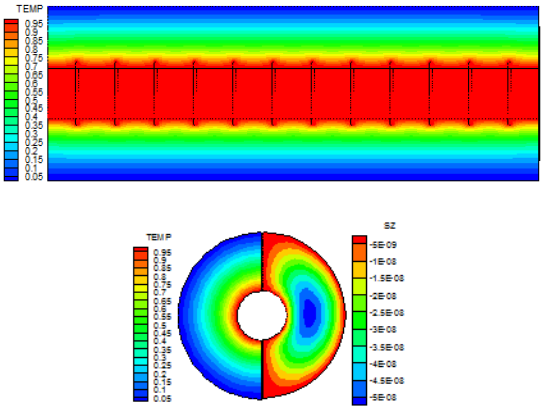

Fig. 3 Isotherm and streamlines for Ra=10, φ=0, Rr=0.293

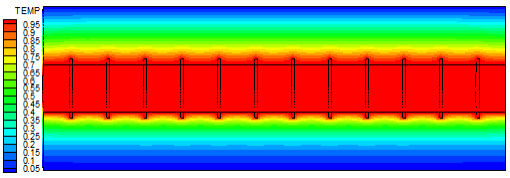

5. RESULTS AND DISCUSSION

5.1 Isotherms and Streamlines Field

A contour map form used to illustrate the dimensionless temperature distribution (isotherms) and the streamlines within the enclosure. To study the temperature distribution, a section in (Z-R) plane along the length of the annulus was selected and the other section in the (R-ϕ) plane. In Fig.3 to Fig.9 the contours of the isotherms and streamlines are shown for different values of Rayleigh number, volume fraction and radius ratios. It is observed that for pure fluid (volume fraction φ=0), isotherms shift towards the outer (cold) wall as the modified Rayleigh number increased. Increase Ra^* and/or decrease in radius ratio result an increase in heat transfer so a thicker cold layer near the bottom wall and a high temperature field near the top wall is observed. When Ra^* increase a swell of the isothermal lines can observed which means a low Nu on the inner hot wall and a high Nu on the outer cold wall. When the radius ratio Rr decrease an increase in temperature is observed much slower near the cold wall and much faster near the hot wall. This further indicates that the sink temperature for the boundary layer on the hot wall reduces as the curvature effects increase. For all cases the waviness in temperature distribution is due to the existence of the fins**.** Far away from the inner cylinder, the isothermal lines are deformed from their conductive pattern, and become curvilinear indicating that an ascending and descending convective flows occur. The streamlines illustrate the contour as unicellular of negative value at center and positive at the boundaries.

Adding nanoparticles cause to enhance heat transfer as shown in Fig. 6 and Fig. 7 where it is clear that the isothermal lines in the upper region of the cylinder abate and come close to the wall, while the cold region in the lower half of the cylinder widens because the temperature decrease in this region. Decreasing the radius ratio which means increasing the gap between the cylinders for φ=0.365 as shown in Fig. 8 and for φ=0.435 in Fig. 9 illustrate that the region will be cold and a definite enhancement in heat transfer will be occur

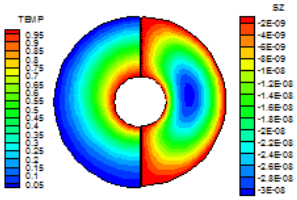

Fig. 4 Isotherm and streamlines for Ra=10, φ=0.5, R=0.293

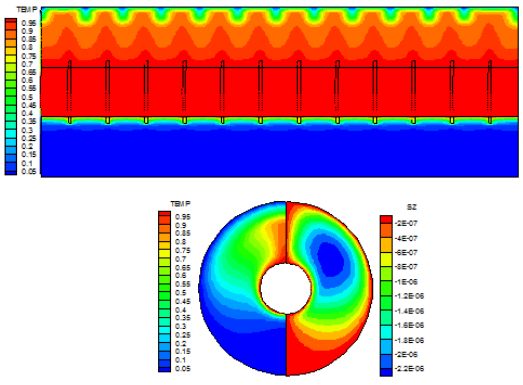

Fig. 5 Isotherm and streamlines for Ra=800, φ=0, Rr=0.293

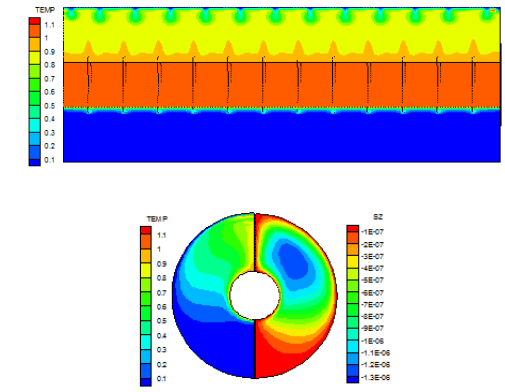

Fig. 6 Isotherm and streamlines for Ra=800, φ=0.3, Rr=0.293

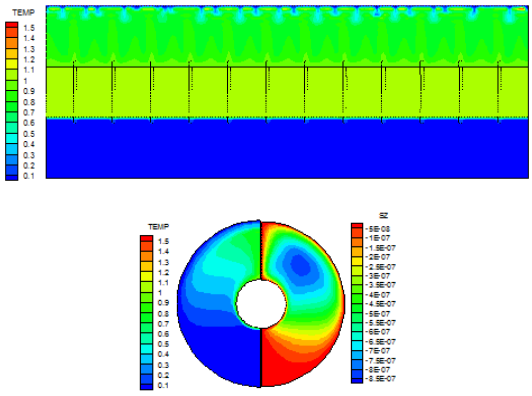

Fig. 7 Isotherm and streamlines for Ra=800, φ=0.5, Rr=0.293

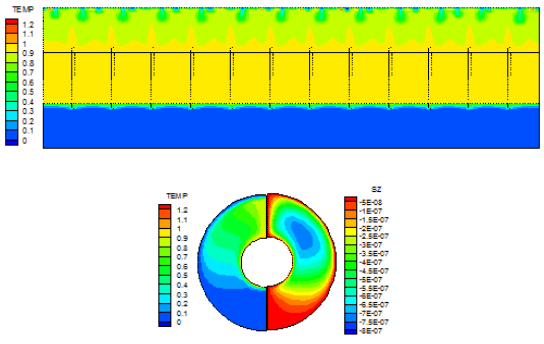

Fig. 8 Isotherm and streamlines for Ra=800, φ=0.5, Rr=0.365

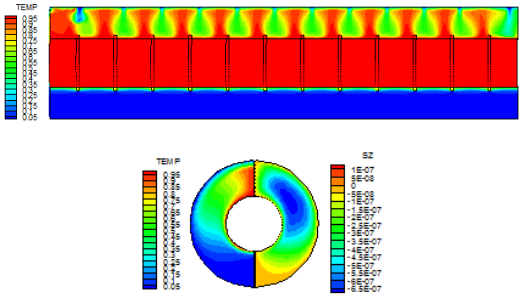

Fig. 9 Isotherm and streamlines for Ra=800, φ=0.5, Rr=0.435

5.2 Variation of Local and Average Nusselt Number

Distribution of local Nusselt number along the cylinder length for various radius ratios and volume fraction are shown in Fig. 10 to Fig. 13.

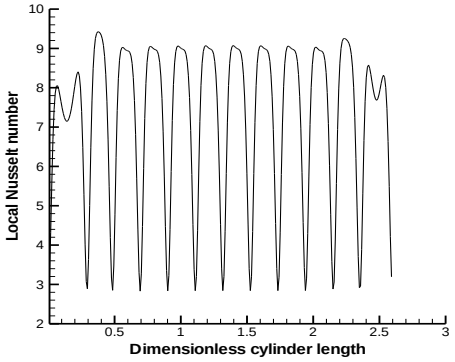

Fig.10 Variation of Nu $_{Local}$ along the cylinder length or Ra=800, φ = 0 and Rr=0.293

Comparing Fig. 10 for pure water with Fig. 11 after adding nanoparticles with φ=0.5, it is clear that there is significant enhance in heat transfer with no uniformity in the distribution of the local Nusselt number. The wavy distribution is due to the existing of the fins on the inner cylinder.

Increasing the radius ratio (which means a reduction in the gap between the two cylinders) as shown in Fig. 12 and Fig. 13, it is clear that as the gap decrease (Rr increase) the heat transfer decrease

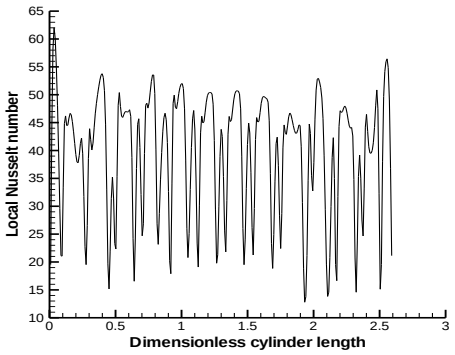

Fig.11 Variation of Nu $_{Local}$ along the cylinder length or Ra=800, φ = 0.5 and Rr=0.293

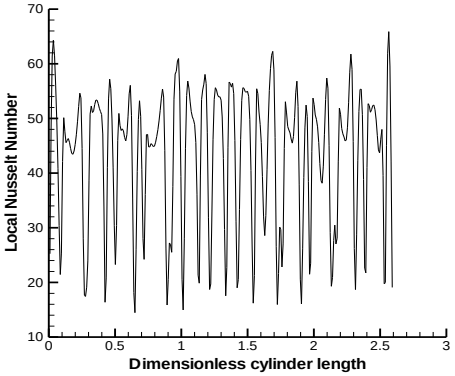

Fig. 12 Variation of Nu $_{Local}$ along the cylinder length or Ra=800, φ = 0.5 and Rr=0.365

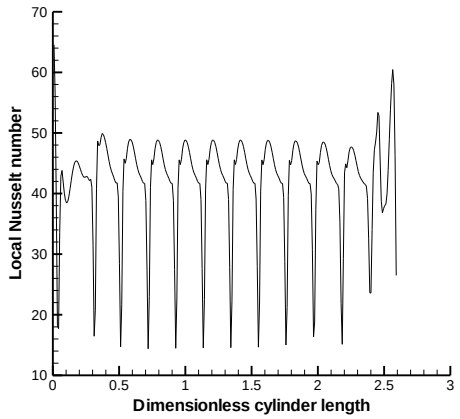

Fig. 13 Variation of Nu $_{Local}$ along the cylinder length or Ra=800, φ = 0.5 and Rr=0.435

Distribution of local Nusselt number along the circumstance of the of cold and hot cylinders respectively are shown in Fig. 14 to Fig. 21 for different volume fraction of nanofluid and radius ratios of the cylinders. The local Nusselt number on the cold wall had an increasing trend from (ϕ= 0˚) to (ϕ =180˚), where the highest values were reached. There were three regions which could be distinguished.

First region at (0˚ ≤ ϕ ≤ 50˚), where the local Nusselt number was relatively constant since the inner boundary layer of relative uniform thickness (see isotherms) and gave a little variation in local Nusselt number distribution.

Second region at (50˚ ≤ ϕ ≤ 140˚), where the local Nusselt number loosed the uniformity and a large gradient in its distribution could be observed and this is because the inner boundary layer got thicker in this region since heat removal by fluid decrease as the fluid ascend up.

Third region at (140˚ ≤ ϕ ≤ 180˚), where the local Nusselt number approached to its maximum values this was due to the formation of plume in this region. Formation of the plume occurred where the two convective currents coming from the two annulus halves, impinging with each other and moving together upward without mixing, leaving a relatively stagnant region under impinging point. This behavior is roughly similar for most of modified Rayleigh number whereas the behavior of the hot wall is to decrease from (ϕ= 0˚) to (ϕ = 180˚).

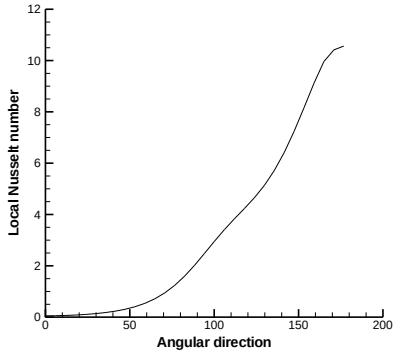

Fig.14 Variation of Nu $_{Local}$ in angular direction on the cold cylinder for Ra=800, φ = 0 and Rr=0.293

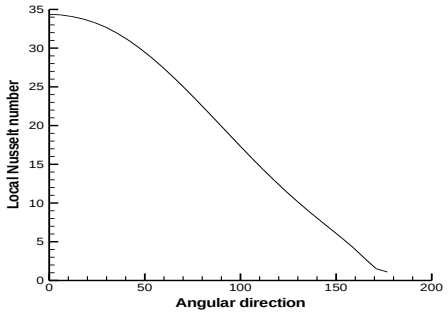

Fig.15 Variation of Nu $_{Local}$ in angular direction on the hot cylinder for Ra=800, φ = 0 and Rr=0.293

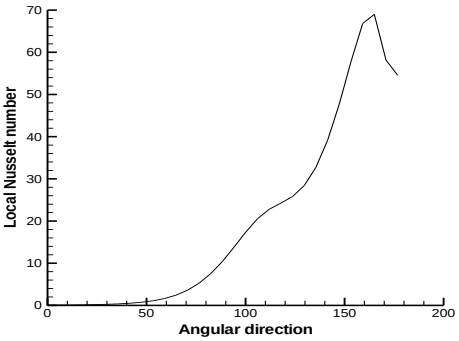

Fig.16 Variation of Nu $_{Local}$ in angular direction on the cold cylinder for Ra=800, φ = 0.5 and Rr=0.293

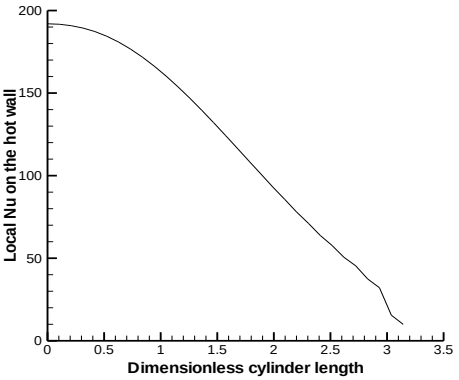

Fig.17 Variation of Nu $_{Local}$ in angular direction on the hot cylinder for Ra=800, φ = 0.5 and Rr=0.293

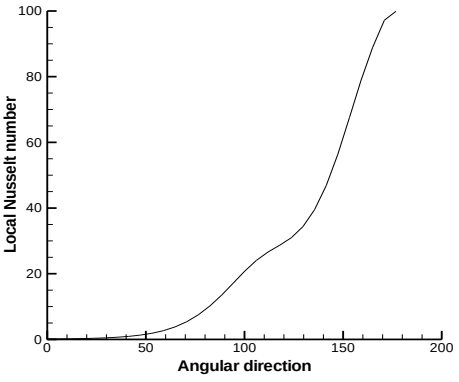

Fig.18 Variation of Nu $_{Local}$ in angular direction on the cold cylinder for Ra=800, φ = 0.5 and Rr=0.365

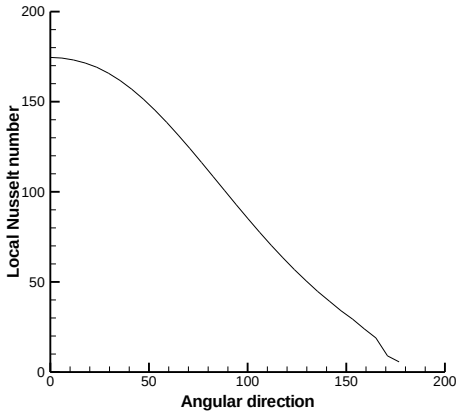

Fig.19 Variation of Nu $_{Local}$ in angular direction on the hot cylinder for Ra=800, φ = 0.5 and Rr=0.365

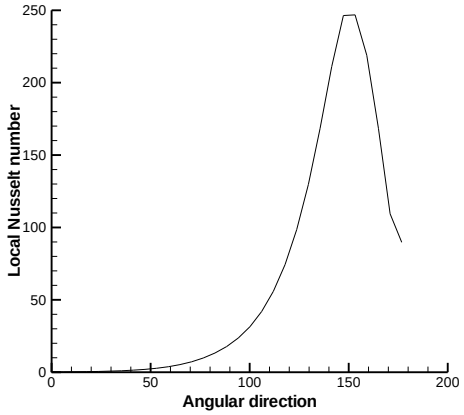

Fig.20 Variation of Nu $_{Local}$ in angular direction on the cold cylinder for Ra=800, φ = 0.5 and Rr=0.435

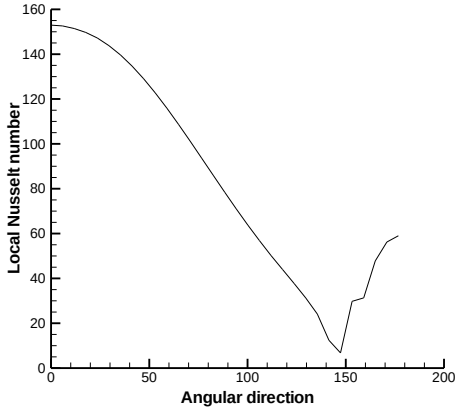

Fig.21 Variation of Nu $_{Local}$ in angular direction on the hot cylinder for Ra=800, φ = 0.5 and Rr=0.435

5.3 Effect of other Parameters

Fig. 22 and Fig. 23 show the variation of the average Nusselt number on the cold and hot cylinders respectively with Ra^* for different radius ratios. These figures show that for any radius ratio, the average *Nu* increased with increasing Ra^*. These values increased as *Rr* decrease due to the enlarge of the gap between the two cylinders.

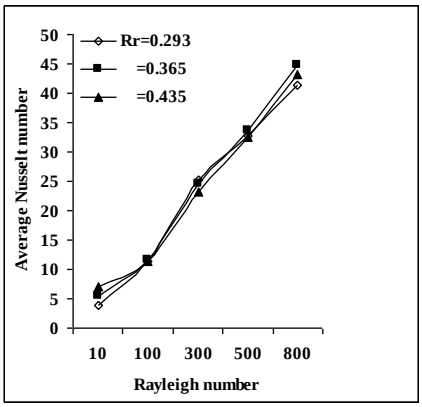

Fig.22 Variation of Nu $_{Average}$ with Ra* for φ = 0.5 and different Rr on the cold cylinder

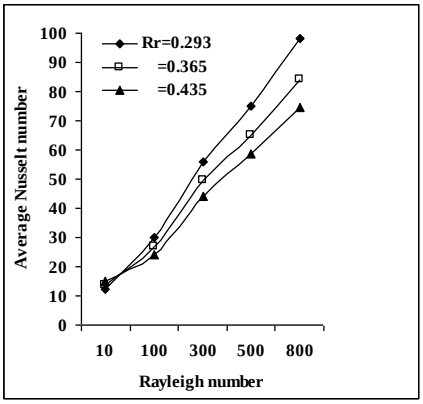

Fig. 23 Variation of Nu $_{Average}$ with Ra* for φ = 0.5 and different Rr on the hot cylinder

For cold cylinder with Ra*=800, adding nanoparticles of a volume fraction equal 0.5 cause to increase the average Nu by 450% as shown in Fig. 24 for Rr=0.293 and 519.6 % increase in average Nu for Rr=0.365 and for Rr=0.435 the % increase in the average Nu is 536.33. For the hot cylinder with Ra*=800, adding nanoparticles by 0.5 a volume fraction cause a deviation in the average Nu by 489.5% as shown in Fig. 25 for Rr=0.293 and 466.77 % for Rr=0.365 and for Rr=0.435 the % deviation in the average Nu is 462.6.

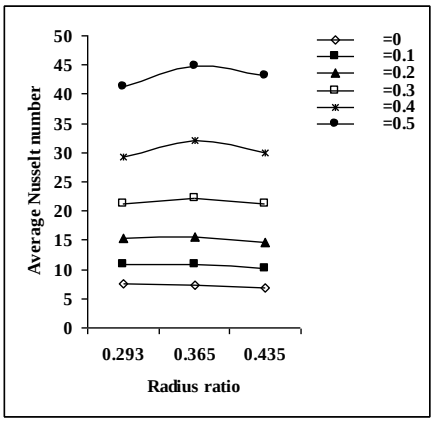

Fig.24 Variation of Nu $_{Average}$ with Rr on the cold cylinder for Ra=800

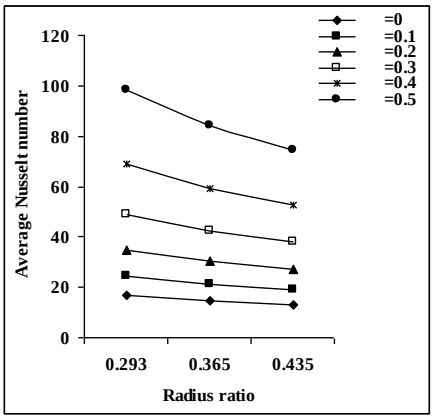

Fig. 25 Variation of Nu $_{average}$ with Rr on the hot cylinder for Ra=800

Fig. 26 to Fig. 31 present the variation of average Nusselt number on the cold and hot cylinders respectively with modified Rayleigh number for different values of volume fraction and radius ratios. The figures show that the heat transfer increases almost monotonically with increasing the volume fraction for all Ra^*. As volume fraction of nanoparticles increases, the increase in average Nusselt number becomes larger especially at higher Ra^* due to increasing of domination of convection heat transfer mode. Effect of nanoparticles on enhancement of heat transfer at high Ra^* is more significant than that at low Ra^*. As the radius ratio decrease which means larger gap between the cylinders, the heat transfer increase.

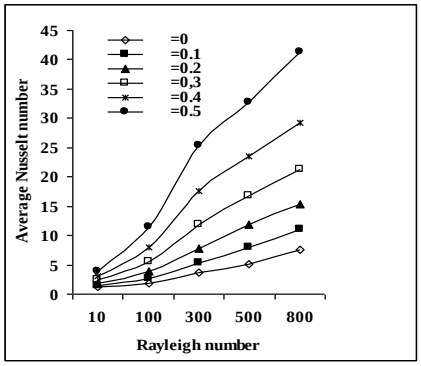

Fig.26 Variation of Nu $_{average}$ with Ra^* on the cold cylinder for Rr=0.293

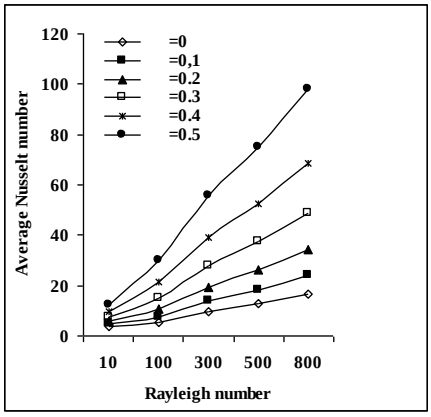

Fig.27 Variation of Nu $_{average}$ with Ra^* on the hot cylinder for Rr=0.293

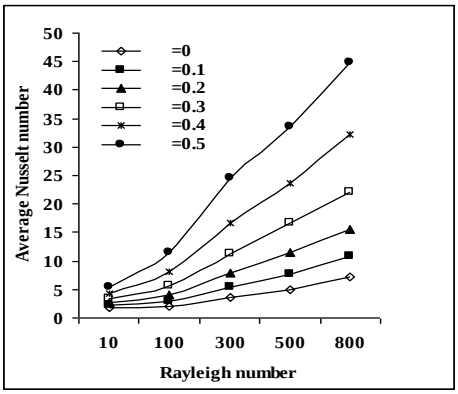

Fig.28 Variation of Nu $_{average}$ with Ra^* on the cold cylinder for Rr=0.365

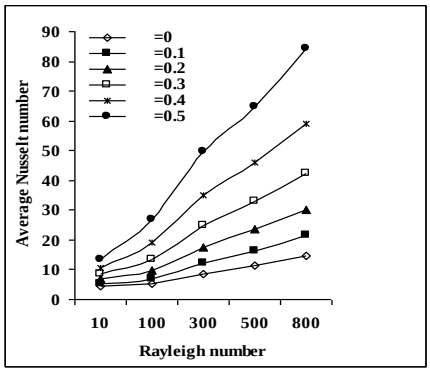

Fig.29 Variation of Nu $_{average}$ with Ra^* on the hot cylinder for Rr=0.365

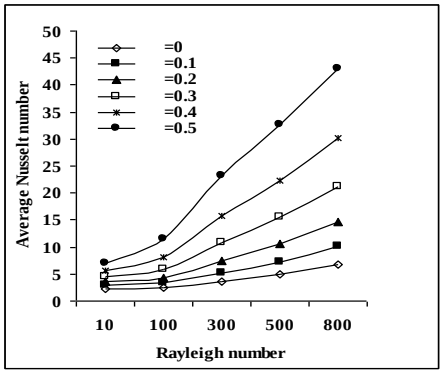

Fig.30 Variation of Nu $_{average}$ with Ra^* on the cold cylinder for Rr=0.435

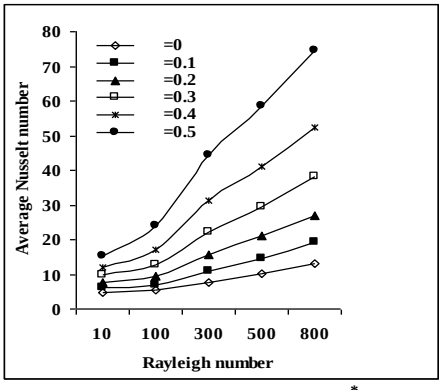

Fig.31 Variation of Nu $_{average}$ with Ra^* on the hot cylinder for Rr=0.435

A correlation for Nu in terms of Ra, φ and Rr, has been developed for outer cold cylinder as follow:

$$Nu = 1.3577 \frac{Ra^{0.407}\varphi^{0.754}}{Rr^{1.554}}$$

6. CONCLUSIONS

The following major conclusions can be drawn from the experimental and numerical study:

1. Increase Ra^* and/or decrease in radius ratio result an increase in heat transfer
2. For cold cylinder with Ra^*=800, adding nanoparticles with a volume fraction equal 0.5 cause to increase the average Nu by 450% for Rr=0.293 and 519.6 % increase in average Nu for Rr=0.365 and for Rr=0.435 the % increase in the average Nu is 536.33
3. For the hot cylinder with Ra^*=800, adding nanoparticles by 0.5 a volume fraction cause an increase in the average Nu by 489.5% for Rr=0.293 and 466.77 % for Rr=0.365 and for Rr=0.435 the % deviation in the average Nu is 462.6.
4. Effect of nanoparticles on enhancement of heat transfer at high Ra^* is more significant than that at low Ra^*.
5. Extension of the present work is recommended for a future work to take other configurations to investigate the enhancement in the heat transfer and use another types of nanoparticles for the purpose of comparison with this research.

7. REFERENCES

[1] D.A. Nield, A. Bejan, Convection in Porous Media, third ed., Springer, New York, 2006.

[2] D. Ingham, I. Pop, Transport Phenomena in Porous Media, vol. III, Elsevier, Oxford, 2005.

[3] I. Pop, D.B. Ingham, Convective Heat Transfer: Mathematical and Computational Modeling of Viscous Fluids and Porous Media, Pergamon, Oxford, 2001.

[4] F. Hakan, Oztop, Eiyad Abu-Nada, Numerical study of natural convection in partially heated rectangular enclosures filled with nanofluids, International Journal of Heat and Fluid Flow 29 (2008) 1326–1336

[5] Syakila Ahmad, Ioan Pop, Mixed convection boundary layer flow from a vertical flat plate embedded in a porous medium filled with nanofluids, International communication in Heat and Mass transfer 37 (2010) 987-991.

[6] Kaustubh Ghodeswar, Natural Convectopn in a Porous Medium Saturated by Nanofluid, M.Sc. thesis, Cleveland State University, December, 2010.

[7] Dalia Sabina Cimpean, Ioan Pop, Fully developed mixed convection flow of a nanofluid through an inclined channel filled with a porous medium, International communication in Heat and Mass transfer 55 (2012) 907-914.

[8] H. Saleh, R. Roslan, I. Hashim, Natural convection heat transfer in a nanofluid-filled trapezoidal enclosure, International Journal of Heat and Mass Transfer 54 (2011) 194–201

[9] R. Nazar · L. Tham · I. Pop · D. B. Ingham, Mixed Convection Boundary Layer Flow from a Horizontal Circular Cylinder Embedded in a Porous Medium Filled with a Nanofluid, Transp Porous Med (2011) 86:517–536

[10] Mina Shahi, Amir Houshang Mahmoudi, Farhad Talebi, A numerical investigation of conjugated-natural convection heat transfer enhancement of a nanofluid in an annular tube driven by inner heat generating solid cylinder, International communication in Heat and Mass transfer 38 (2011) 533-542

[11] M. Esmaeilpour, M. Abdollahzadeh, Free convection and entropy generation of nanofluid inside an enclosure with different patterns of vertical wavy walls, International Journal of Thermal Science 52 (2012)127-136

[12] Wang Bu – Xuan and Zhang Xing, "Natural Convection in Liquid Saturated Porous Media Between Concentric Inclined Cylinders" Int. J. Heat and Mass Transfer Vol. 33. No 5, pp. 827-833, 1990.

[13] Fukuda K., Takata Y., Hasegawa S., Shimomura H. and Sanokawa K., "Three – Dimensional Natural Convection in a Porous Medium Between Concentric Inclined Cylinders", Proc. 19th Natl Heat Transfer Conf., Vol. HTD – 8, pp. 97 – 103, 1980

[14] Ramón L. F. and Sergio G. M., "Three Dimensional Natural Convection in Finned Cubical Enclosure", Int. J. of Heat and Fluid Flow, Vol. 28, pp. 289-298, 2007.